

Correspondence

Eckard Wimmer
ewimmer@ms.cc.sunysb.edu

Analysis of the cloverleaf element in a human rhinovirus type 14/poliovirus chimera: correlation of subdomain D structure, ternary protein complex formation and virus replication

Elizabeth Rieder,[†] Wenkai Xiang,[‡] Aniko Paul and Eckard Wimmer

Department of Molecular Genetics and Microbiology, School of Medicine, Stony Brook University, Stony Brook, NY 11794-5222, USA

[†]**Present address:** US Department of Agriculture, Agricultural Research Service, Plum Island Animal Disease Center, Greenport, NY 11944, USA.

[‡]**Present address:** The Wharton School of the University of Pennsylvania, Philadelphia, PA, USA.

Received 27 November 2002

Accepted 15 April 2003

Ahead-of-print 14 May 2003

RNA genomes of enteroviruses and rhinoviruses contain a 5'-terminal structure, the cloverleaf (CL), which serves as signal in RNA synthesis. Substitution of the poliovirus [PV1(M)] CL with that of human rhinovirus type 2 (HRV2) was shown previously to produce a viable chimeric PV, whereas substitution with the HRV14 CL produced a null phenotype. Fittingly, the HRV14 CL failed to form a complex with PV-specific proteins 3CD^{pro}–3AB or 3CD^{pro}–PCBP2, considered essential for RNA synthesis. It was reported previously (Rohll *et al.*, *J Virol* 68, 4384–4391, 1994) that the major determinant for the null phenotype of a PV/HRV14 chimera resides in subdomain Id of the HRV14 CL. Using a chimeric PV/HRV14 CL in the context of the PV genome, stem–loop Id of HRV14 CL was genetically dissected. It contains the sequence C₅₇UAU₆₀-G, the underlined nucleotides forming the loop that is shorter by 1 nt when compared to the corresponding PV structure (UUGC₆₀GG). Insertion of a G nucleotide to form a tetra loop (C₅₇UAU₆₀GG₆₁) did not rescue replication of the chimera. However, an additional mutation at position 60 (C₅₇UAC₆₀GG₆₁) yielded a replicating genome. Only the mutant PV/HRV14 CL with the UAC₆₀G tetra loop formed ternary complexes efficiently with either PV proteins 3CD^{pro}–3AB or 3CD^{pro}–PCBP2. Thus, in the context of PV RNA synthesis, the presence of a tetra loop in subdomain D of the CL per se is not sufficient for function. The sequence and, consequently, the structure of the tetra loop plays an essential role. Biochemical assays demonstrated that the function of the CL element and the function of the *cis*-acting replication element in the 3D^{pol}–3CD^{pro}-dependent uridylylation of VPg are not linked.

INTRODUCTION

The genomes of plus-strand RNA viruses harbour a multitude of genetic information, directing uncoating, protein synthesis, modulation of gene expression, genome replication and encapsidation, and probably more. Signals encoded in viral RNA genomes are often presented in higher order structures, the complexity of which is not understood. The discovery and characterization of these signals and the mechanisms by which they transmit their information on virus proliferation is one of the biggest challenges in RNA virus research (Wimmer, 1997).

Genomes of the plus-strand RNA virus members of the family *Picornaviridae* are examples of relatively small replicating units (~7500 nt) that are filled with structural information. The genomes of member viruses of two genera of the *Picornaviridae*, *Enterovirus* and *Rhinovirus*, are related more closely to each other than to other genera of the *Picornaviridae* and they have been studied intensely for RNA replication signals. Currently, four such signals have been identified: the 5'-terminal cloverleaf (CL), the *cis*-acting replication element (*cre*), the 3'-terminal heteropolymeric region and the 3'-terminal poly(A) tail (Agol *et al.*, 1999; Paul, 2002; Xiang *et al.*, 1997). The IRES, located in the 5'NTR, might also be added. Apart from genetic evidence, however, there are no biochemical data to suggest that the IRES is involved directly in RNA synthesis (Agol *et al.*, 1999; Zhao & Wimmer, 2001).

In this study, we have focused on the structure/function relationship of the 5'-terminal CL in poliovirus (PV) RNA synthesis. This structure (Fig. 1), first proposed by Rivera *et al.* (1988), has been shown to form a ribonucleoprotein (RNP) complex involved in genome replication (Andino *et al.*, 1990, 1993). Key to the formation of the RNP is the recognition of the CL by the viral proteinase and RNA-binding protein 3CD^{pro} (Andino *et al.*, 1990, 1993). Together with either the cellular poly(C)-binding protein (PCBP2 and PCBP1) (Blyn *et al.*, 1996; Gamarnik & Andino, 1997; Parsley *et al.*, 1997; Walter *et al.*, 2002) or the viral RNA-binding protein 3AB, the precursor for VPg (Harris *et al.*, 1994; Paul *et al.*, 1994; Xiang *et al.*, 1995a, b), the CL–3CD^{pro} complex can also form a ternary complex. It was observed that the 3C^{pro} domain of 3CD^{pro} carries the RNA recognition signal (Andino *et al.*, 1990; Blair *et al.*, 1998) and this activity could be modulated by 3D^{pol} (Cornell & Semler, 2002). However, for PV, it is the precursor 3CD^{pro} which possesses the higher affinity to the CL (Harris *et al.*, 1994). 3C^{pro}–CL RNA complexes have been described for other picornaviruses as well, including rhinovirus and hepatitis A virus (Leong *et al.*, 1993; Kusov & Gaus-Muller, 1997). Ternary complex formation and viral RNA synthesis co-vary; that is, if the CL is modified such that it cannot bind the above-mentioned proteins, there will be no viral RNA synthesis. Hence, this modification results in a lethal phenotype. Genetic and biochemical evidence suggests that PCBP2 binds to subdomain B of the CL, while 3CD^{pro} binds to subdomain D (Andino *et al.*, 1990, 1993; Gamarnik & Andino, 1997; Parsley *et al.*, 1997). PV protein 3AB, on the other hand, is a non-specific RNA-binding protein (Paul *et al.*, 1994) and, thus, it will bind CL RNA non-specifically in

the absence of competitor RNA. In the presence of as much as a 1000-fold molar excess of competitor RNA, however, 3AB will form the ternary complex CL–3CD^{pro}–3AB with high specificity (Harris *et al.*, 1994; Xiang *et al.*, 1995a, b).

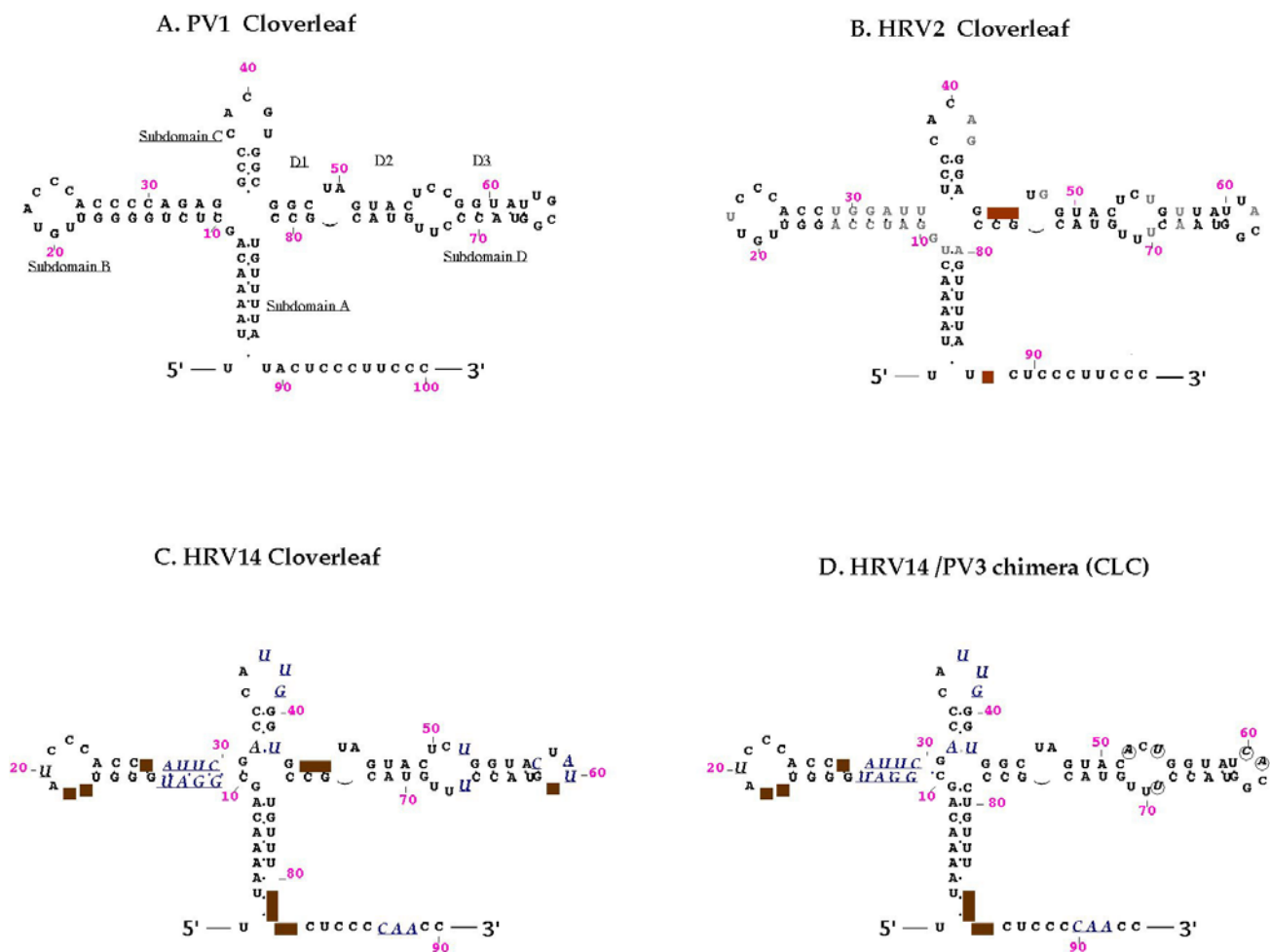


Fig. 1. Comparison of CL homologues. Primary sequences and secondary structures are compared among CL RNAs from (A) PV1, (B) HRV2, (C) HRV14 and (D) HRV14/PV3 (CLC). The naming of each subdomain stem-loop is indicated in (A). Bold letters represent PV1 sequences and identical sequences in HRV2 and HRV14 CLs. Filled rectangles represent PV1 sequences absent in HRV2 and HRV14 CLs. Underlined and italic letters display the sequence differences between HRV14 and PV1. Blue letters display the sequence differences between HRV2 and PV1. Circled letters are PV3 sequences in subdomain D that are different from its PV1 counterpart.

The study of the role of the CL in enterovirus and rhinovirus replication has led to the construction of chimeric genomes in which the replication proteins of one virus species were confronted with the 5'-terminal replication signals of another. Within the genus *Enterovirus*, these experiments involved substitution of the entire 5'-terminal region of PV with that of coxsackievirus B3 (CVB3) (Johnson & Semler, 1988), the exchange of 220 nt of the CVB3 genome with that of PV (Zell *et al.*, 1995) or exchanges of CVB3 5'-terminal sequences with segments of different lengths of the bovine enterovirus 5'NTR (Zell *et al.*, 1999). Rohll *et al.* (1994) and Xiang *et al.* (1995b) performed exchanges between PV

and members of the genus *Rhinovirus*. In most cases, viable chimeras were obtained with replication phenotypes, including host range phenotypes. The exception was the replacement of the PV CL with that of human rhinovirus type 14 (HRV14). In the context of PV type 3 (Leon) [PV3(L)] (Rohll *et al.*, 1994) or PV1 (Mahoney) [PV1(M)] (Xiang *et al.*, 1995b), this exchange proved lethal. Surprisingly, the replacement of the PV1(M) CL with that of HRV2 yielded a viable chimera (Xiang *et al.*, 1995b).

The structure of all enterovirus and rhinovirus CLs is similar (Zell *et al.*, 2002; and references therein) (Fig. 1); they consist of four subdomains, stem-loop B being the most stable (Andino *et al.*, 1990; Larsen *et al.*, 1981; Rivera *et al.*, 1988). Rohll *et al.* (1994) have reported that substitution of subdomain D in the HRV14 CL with that of PV3(L) can rescue the replication function of the HRV14/PV3(L) chimera. This observation has led us to focus on sequence parameters of subdomain D in the HRV14 CL and relating genetically changed versions of subdomain D with the ability to form ternary complexes and replication phenotypes. Although the structure of subdomain D of the HRV14 CL loop consists only of 3 nt (the loop in the subdomains D of the other viruses have 4 nt), the formation of tetra loops in this region is still evident (Fig. 1 and see Fig. 4B). Addition of a G residue to the loop of HRV14 subdomain D rescued weakly the ability of this CL to form a ternary complex, with either 3CD^{pro}-3AB or 3CD^{pro}-PCBP2, but this characteristic was not sufficient to rescue replication in the context of the PV genome. In addition, nucleotide changes were required to yield a proliferating HRV14/PV genome.

While this work was in progress, Zell *et al.* (2002) published an interesting study in which binding parameters of the CVB3 3C^{pro} proteinase (the RNA-binding domain of 3CD^{pro}) to subdomains D of CVB3, PV1(M), HRV2, bovine enterovirus and a modified version of HRV14 were reported. Zell and co-workers concluded that the presence of a tetra loop in subdomain D is sufficient to bind the viral protein and that a defined sequence of this loop is less important, if at all. We agree with the importance of the tetra loop in subdomain D of the CLs of most enteroviruses and rhinoviruses. However, we present evidence that, in the context of PV, the sequence of the tetra loop also plays an essential role in protein binding and replication. Moreover, we show that the function of the CL and the function of the *cre* (Gerber *et al.*, 2001; Goodfellow *et al.*, 2000; Lobert *et al.*, 1999; Mason *et al.*, 2002; McKnight & Lemon, 1996, 1998) in the *in vitro* 3D^{pol}-3CD^{pro}-dependent uridylylation (Gerber *et al.*, 2001; Paul *et al.*, 2000; Rieder *et al.*, 2000; Yin *et al.*, 2003) of VPg are not linked.

METHODS

Plasmid constructions. Plasmid 5'-d-REP is a cDNA replicon of PV3, carrying a hybrid HRV14 CL and subdomain D exchanged by the corresponding elements of PV3, kindly provided by J. W. Almond (Rohll *et al.*, 1994). Using this replicon, a DNA fragment corresponding to the CL region was amplified

by PCR, with *NaeI* and *XmaI* sites flanking the ends. The PCR fragment and the plasmid pPV1(M) (referred to as pPVS100 in Xiang *et al.*, 1995b) were digested with *NaeI/XmaI* and ligated together to generate pCLCPV. A similar strategy was used to generate the mutants M1-, M2- and M3-R14PV, by replacing the *NaeI-XmaI* fragment in pPV1(M) with the *NaeI-XmaI* fragment generated by PCR using mutagenic primers. The sequences of the mutant primers were

5'-GGGTGTAGTACTCTGGTACTATGGTACCTTTGTACGCC-3' for M1-R14PV,

5'-GGGTGTAGTACTCTGGTACTACGGTACCTTTGTACGCC-3' for M2-R14PV

and 5'-GGGTGTAGTACTCTGGTATTACGGTACCTTTGTACGCC-3' for M3-R14PV. All sequences derived from PCR were verified by sequencing. To construct pR2LEP and pR14LEP, the *NaeI-NheI* fragment in a dicistronic Luciferase/PV genome PLEP [(PV)5'NTR-Luc-(EMCV)IRES-(PV)P1,2,3-3'NTR,poly(A)] (Fig. 2A) (Alexander *et al.*, 1994) was replaced with those from pR2PV and pR14PV PLEP (Xiang *et al.*, 1995b), respectively. pT7HRV2, used to derive pR2PV, was a generous gift from E. Kuechler, Institute of Medical Biochemistry, Vienna, Austria (GenBank accession number X02316). Subsequently, pCLCLEP was constructed by switching the *NaeI-XmaI* fragment in pR2LEP for the one in pCLCPV.

***In vitro* transcription and translation.** Prior to T7 RNA polymerase transcription, pPV1(M) and its derivatives were linearized with *EcoRI*, whereas PLEP and its derivatives were linearized with *AatII*. The condition of transcription has been described before (van der Werf *et al.*, 1986). RNAs used in electrophoretic mobility shift assays (EMSAs) were transcribed *in vitro* from linearized pPV1(M) (wt, *XmaI* cut) or its mutant derivative plasmids in the presence of [α -³²P]UTP, gel purified and quantified based on radioisotope-specific activity. *In vitro* RNA translations were performed using HeLa cell-free extracts, as described previously (Molla *et al.*, 1991).

RNA transfection, plaque assay and one-step growth curve. RNA transfections were performed with R19 HeLa cells by the DEAE-Dextran method, as described elsewhere (Rieder *et al.*, 2000). Supernatants harvested from transfected cells were subjected to plaque assays (Molla *et al.*, 1991). For the one-step growth curve assays, R19 HeLa cell monolayers in 35 mm plastic culture dishes were infected at an m.o.i. of 10, unless indicated otherwise. At various time-points post-infection, the cells were harvested and the titres of the viruses were determined by plaque assay.

Viral RNA isolation and RT-PCR. Total RNA was isolated from infected cells using Trizol (Life technologies). First-strand cDNAs were synthesized using a random deoxynucleotide hexamer and Moloney murine leukaemia virus reverse transcriptase (Life Technologies). cDNAs were amplified with specific pairs of primers by standard PCR procedures and sequenced directly.

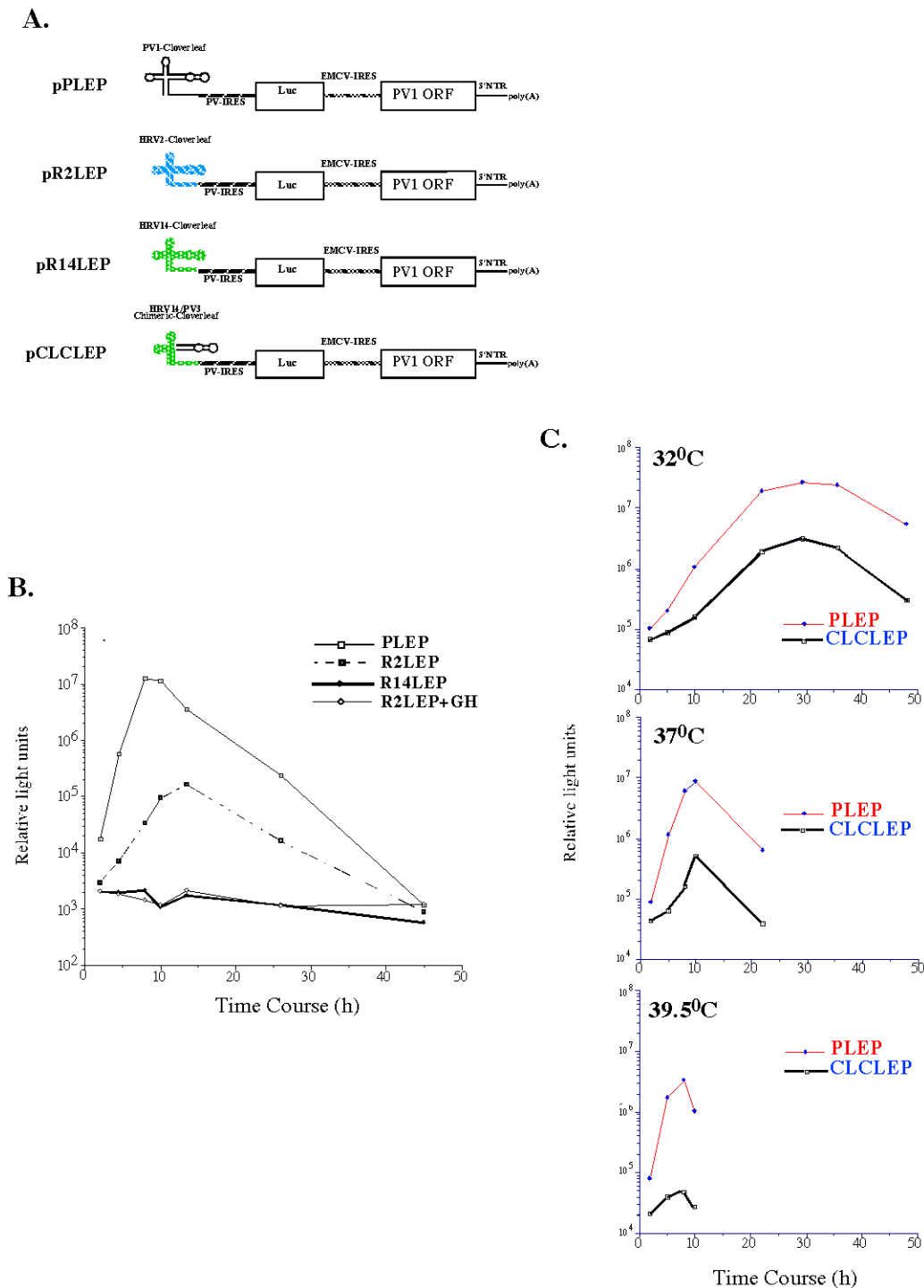


Fig. 2. Schematic depiction and replication activities of dicistronic constructs driven by different CL elements. (A) Dicistronic constructs were made in which the PV1 and encephalomyocarditis virus (EMCV) IRESs initiate the translations of luciferase and PV1 P1–P3 proteins, respectively. All four constructs are identical, except that the 5' CL RNA is from PV1, HRV2 or HRV14 or from the HRV14/PV3 (CLC) chimera. (B) Determination of luciferase activity. Transcript RNA derived from constructs depicted in (A) were transfected into HeLa cell monolayers and, at each time-point, luciferase activities were determined. As a control for background activity, R2LEP-transfected cells were treated with 2 mM guanidine/HCL (GH) and the luciferase activity was measured. (C) PLEP and CLCLEP transcripts were transfected into cells, which were then incubated at three different temperatures. At each temperature, the luciferase activities corresponding to both transfecting RNAs were compared.

Luciferase assay. Luciferase assays were performed using protocols described previously. Briefly, about 20 μg RNA transcript was used to transfect 10^6 HeLa cell monolayers. The RNA transfection was carried out in the presence of 2 U RNase inhibitor μl^{-1} (Boehringer Mannheim). The cells were then incubated at 32, 37 or 39.5 °C. At each time-point, the cells were washed with cold HBSS buffer and lysed with 200 μl lysis buffer (10 mM Tris/HCl pH 7.5, 1 mM EDTA, 0.5 % NP-40 and 100 mM NaCl). The suspension was centrifuged at 2000 r.p.m. in a Sorvall RC-5B centrifuge and the supernatant was collected. The relative luciferase activity was measured in an Optocomp I luminometer (MGM Instruments).

Dot blot hybridization. Viral RNA transcripts produced *in vitro* (5 μg) were transfected into 35 mm dishes of R19 HeLa cells. At several time-points after transfection, total RNA was extracted from the cells using Trizol. Digoxigenin (DIG)-labelled minus-strand RNA was synthesized from a *Bam*HI digestion of pBS-2C (a gift from T. Pfister, Cytos Biotechnology AG, Schlieren, Switzerland), corresponding to the 5'-terminal portion of the 2C^{ATPase}-encoding region (nt 4123–4400), using T3 RNA polymerase and a mixture containing DIG-labelled UTP (Roche). The RNA was denatured and blotted onto a nylon membrane (Boehringer Mannheim) pre-soaked with 20 \times SSC (3 M NaCl and 0.3 M sodium citrate, pH 7.0) using a Dot Blotter (Schleicher&Schuell). The RNA was then cross-linked to the membrane in a 1800 Stratalinker. The membrane was incubated with the DIG-labelled RNA in hybridization buffer (50 % formamide, 5 \times SSC, 0.2 % SDS, 0.1 % sodium-lauroylsarcosine and 0.05 mg tRNA ml^{-1}) at 68 °C overnight. Afterwards, the membrane was washed twice in 2 \times wash solution (2 \times SSC and 0.1 % SDS) at room temperature, followed by two washes in 0.5 \times wash solution (0.5 \times SSC and 0.1 % SDS) at 68 °C (15 min each). The membrane was incubated with anti-DIG alkaline phosphatase-conjugated antibody (Roche) and incubated for 5 min. To detect the chemiluminescent signal, the membrane was exposed to a Kodak MR X-ray film.

RNA binding assay. The binding of proteins to the CL was carried out by an RNA mobility shift assay, similar to what was described before (Xiang *et al.*, 1995b). The reaction mixture (25 μl) contained 30 000 c.p.m. [α -³²P]UTP-labelled RNA probes generated by *in vitro* transcription, as described above. The riboprobes were incubated at 45 °C for 30 min prior to the addition to the binding reactions. Protein/RNA mixtures were incubated at 30 °C for 10 min, stopped by the addition of 5 μl 50 % glycerol and loaded on a native 0.5 \times TBE, 5 % polyacrylamide (40:1) gel containing 5 % glycerol. Purified 3AB (Lama *et al.*, 1994), 3CD^{pro} and PCBP2 recombinant proteins [the latter two derived from His-tagged plasmids pET21b/3CD^{pro} (3C^{pro}/H40A) and pET21b/PCBP2; Paul *et al.*, 2000) were used at 0.2, 0.8 and 0.3 μM , respectively. A 15 μg sample of tRNA from Baker's yeast (Boehringer Mannheim) was added as non-specific RNA competitor in each reaction.

VPg uridylylation assay. This assay was similar to that described before (Paul *et al.*, 2000; Rieder *et al.*, 2000). The standard reaction mixture (20 μ l) for VPg uridylylation contained 50 mM HEPES pH 7.6, 3.5 mM MgAc₂, 8 % glycerol, 2.0 μ g genomic RNA template transcribed *in vitro*, 2 μ g synthetic PV VPg, 10 μ M unlabelled UTP, 1 μ g (1 μ M) purified 3D^{pol} and 1 μ Ci [α -³²P]UTP (0.017 μ M) (3000 Ci mmol⁻¹, Dupont NEN). Unless indicated otherwise, 0.7 μ g 3CD^{pro} was added to each reaction. Samples were incubated for 1 h at 30 °C and the reactions were stopped by the addition of 5 μ l gel-loading buffer (Bio-Rad) and analysed by Tris/Tricine/SDS-PAGE (Bio-Rad) with 13.5 % polyacrylamide. Gels were dried at 68 °C for 2 h and autoradiographed (Kodak Biomax MS film). Reaction products were quantified by measuring the amount of [α -³²P]UMP incorporated into the VPgpU and VPgpUpU products (Molecular Dynamics PhosphoImager, Storm 860).

RESULTS

Characterization of PV chimeras containing wt or HRV CLs

Amongst three *cis*-acting elements functioning in genome replication of enteroviruses and rhinoviruses, CL, *cre* and heteropolymeric 3'-terminal NTR with the poly(A) tail, the CLs exhibit the highest degree of structural homology (Gerber *et al.*, 2001; Goodfellow *et al.*, 2000; McKnight & Lemon, 1998; Paul *et al.*, 2000; Pfister & Wimmer, 1999; Rieder *et al.*, 2000; Xiang *et al.*, 1997). We have followed in the past a strategy of exchanging CL elements from one virus species to another in the hope that the chimeric genomes display replication phenotypes open to genetic analysis of the element (Xiang *et al.*, 1995b). We have found that the cognate CL of the PV genome (Fig. 1A) can be exchanged with that of HRV2 (Fig. 1B) to yield a viable chimera, whereas an exchange with the HRV14 CL (Fig. 1C) yielded RNA unable to replicate (Xiang *et al.*, 1995b). Similarly, Rohll *et al.* (1994) reported that the HRV14 CL is incompatible with replication of PV3(L) RNA.

To analyse the kinetics of genome replication of the PV/HRV chimeras, we used dicistronic genomes carrying the luciferase gene. The prototype (PLEP) of such a dicistronic genome [(PV)5'NTR-Luc-(EMCV)IRES-(PV)P1,2,3-3'NTR,poly(A)] (Fig. 2A) was constructed originally by Alexander *et al.* (1994). Although the RNA (PLEP) is too large for encapsidation, it provides a measure of genome replication. Plasmids of the parental construct and two replicons with exchanges of the PV CL with that of HRVs, PV/HRV2 (R2LEP) and PV/HRV14 (R14LEP) (Fig. 2A), were transcribed and the transcript RNAs were transfected into HeLa cells. At different times, luciferase activity was monitored (Fig. 2B). Whereas the parental RNA expresses luciferase activity as long as 30 h or more, R2LEP RNA expressed luciferase at approximately 1 % of PLEP, with a delay in reaching the peak level. Addition of 2 mM guanidine hydrochloride (GH), an inhibitor of PV RNA replication (Wimmer *et al.*, 1993), to R2LEP-

transfected cells suppressed luciferase activity. This observation suggested that the bulk of the signal was produced by replicating RNA and not transfected RNA. In cells transfected with R14LEP RNA, only background levels of luciferase were observed, which confirmed that this RNA is unable to replicate under these conditions.

Rohll *et al.* (1994) made the interesting observation that a HRV14/PV3 chimeric CL in which subdomains A, B and C (the first 42 nt) originated from HRV14 and subdomain D originated from PV3(L) was capable of RNA synthesis. These authors measured PV3 RNA replication by replicon-expressed CAT assays. Making use of this HRV14/PV3(L) chimeric CL (Fig. 1D, named here as CLC) [kindly provided by J. B. Rohll (Department of Microbiology, University of Reading, UK) and J. W. Almond (Aventis Pasteur, Lyon, France)], we constructed viral genomes with the purpose of assaying genome replication and virus production.

Replication of the dicistronic replicon carrying CLC at its 5' end (Fig. 2A, CLCLEP) was apparent, as assayed by luciferase activity (Fig. 2C). Rescue of RNA synthesis by CLC, however, was poor, as compared to a replicon carrying the PV CL (Fig. 2C). At 39.5 °C, the luciferase signal was especially low, an observation that suggested a temperature-sensitive (*ts*) phenotype (Fig. 2C, lower panel).

The replication phenotypes observed with CLCLEP could be due, at least in part, to the complex structure of the dicistronic genomes. Therefore, we replaced the cognate CL of PV1(M) with CLC (Fig. 3A, CLCPV) to generate a proliferating chimeric genome. RNA transcripts of wt PV1(M) or CLCPV were used to transfect R19 HeLa cell monolayers and the cells were incubated at 32, 37 and 39.5 °C. At 37 °C, CPE with wt RNA-transfected cells was apparent after 20 h. In contrast, CLCPV RNA produced CPE only after 72 h, an observation indicative of impaired replication. Indeed, viable virus recovered from the cells transfected with CLCPV RNA at 37 °C yielded virus expressing a minute plaque phenotype (data not shown). In a one-step growth experiment, CLCPV produced virus at 32 and 37 °C, approximately one log lower than the wt construct at the same temperatures (Fig. 3B). Interestingly, replication of CLCPV expressed a very strong *ts* phenotype at 39.5 °C, just as CLCLEP did. Indeed, the yield of CLCPV in a one-step growth experiment was <1 % of that of the wt virus (Fig. 3B). These data confirm that the replacement of subdomain D of the HRV14 CL with that of PV3(L) can rescue CL function. The efficiency of the chimeric CL, however, is poor.

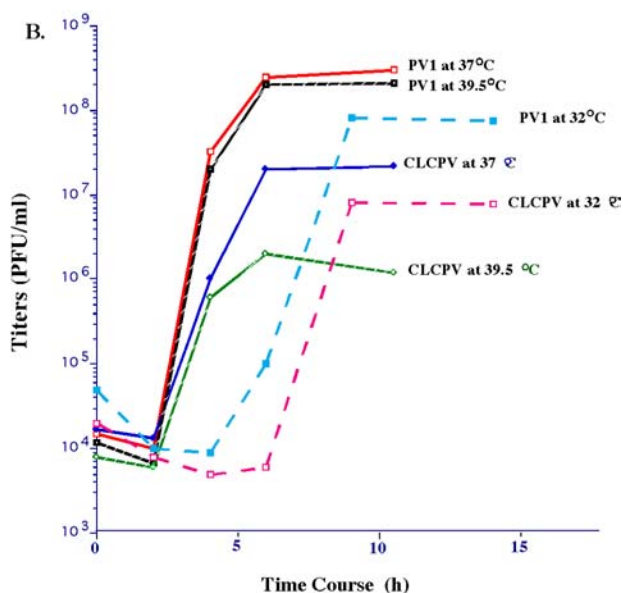
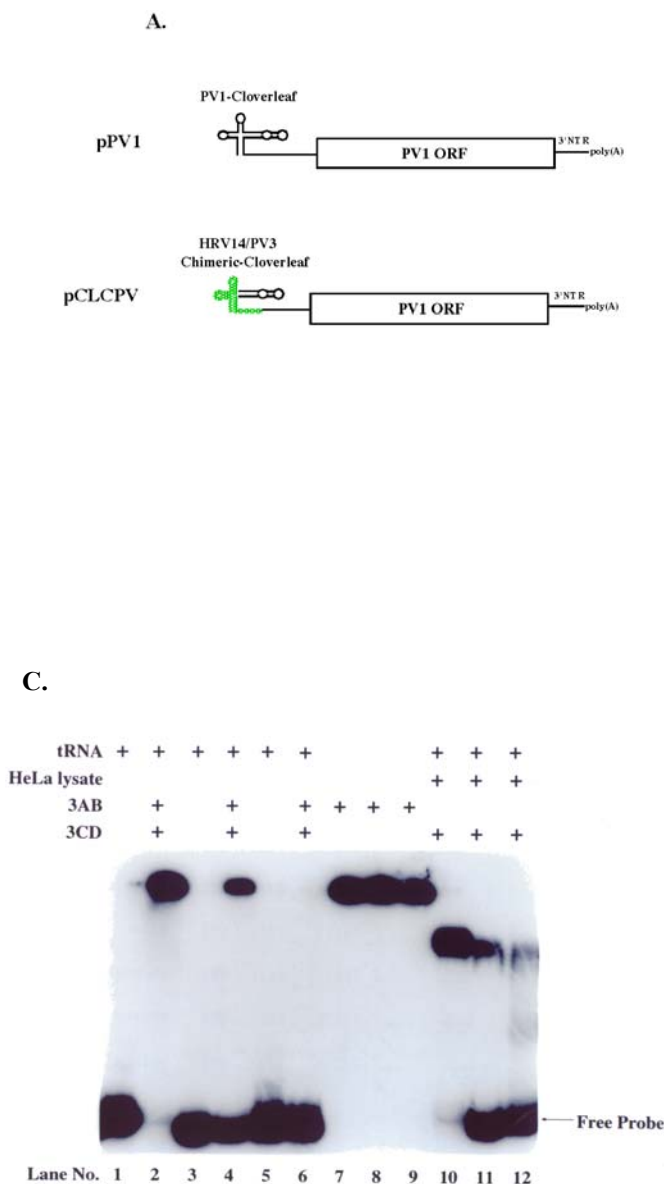


Fig. 3. Characterization of the CLCPV chimeric virus containing a hybrid CL at the 5'NTR. (A) Schematic drawing of the genomic organization of the wt and CLCPV chimera. (B) One-step growth curves of wt and CLCPV viruses at different temperatures. HeLa cells were infected with viruses at an m.o.i. of 10. At various time-points after infection, cells were harvested and the titres of the viruses were determined by plaque assay. (C) RNP-forming activities of different CL RNAs. [³²P]UTP-labelled PV1 (lanes 1, 2, 7 and 10), CLC (lanes 3, 4, 8 and 11) or HRV14 (lanes 5, 6, 9 and 12) CL RNAs were added into each binding reaction. Other factors were also included, as indicated above each lane.

We then investigated protein binding to the different CL structures to determine whether the ability of RNP formation co-varies with replication. The PV polypeptides 3CD^{PRO} and 3AB, known to interact strongly and specifically with PV CL elements (Harris *et al.*, 1994; Xiang *et al.*, 1995a, b), were incubated in the presence of a 1000-fold molar excess of tRNA with [³²P]UTP-labelled CL RNAs of PV1(M), HRV14 and CLCPV. Formation of RNP complexes was then analysed by EMSAs. Most of the PV1(M) CL probe was shifted by 3CD^{PRO}-3AB (Fig. 3C, compare lane 2 with lane 1), an indication of efficient binding. Under the same conditions, very little, if any, HRV14 CL was retarded (Fig. 3C, lane 6). In contrast, the chimeric CL CLC restored the RNP-forming ability, albeit reduced to about 30 % (Fig. 3C, lane 4). The binding reaction was also carried out with PV 3CD^{PRO} and a cytoplasmic extract of uninfected HeLa cells as a source of a cellular factor. The PV1(M) CL shifted in the presence of 3CD^{PRO} and extract (Fig. 3C, lane 10), which is due to the host factor PCBP2 (Blyn *et al.*, 1996; Parsley *et al.*, 1997). Complex formation between 3CD^{PRO} and the cellular extract and binding to CLC was reduced (Fig. 3C, lane 11, estimated to be 30 %), an observation resembling the finding with 3CD^{PRO}-3AB. Surprisingly, the HRV14 probe was also capable of binding 3CD^{PRO}-host factor in the presence of a 1000-

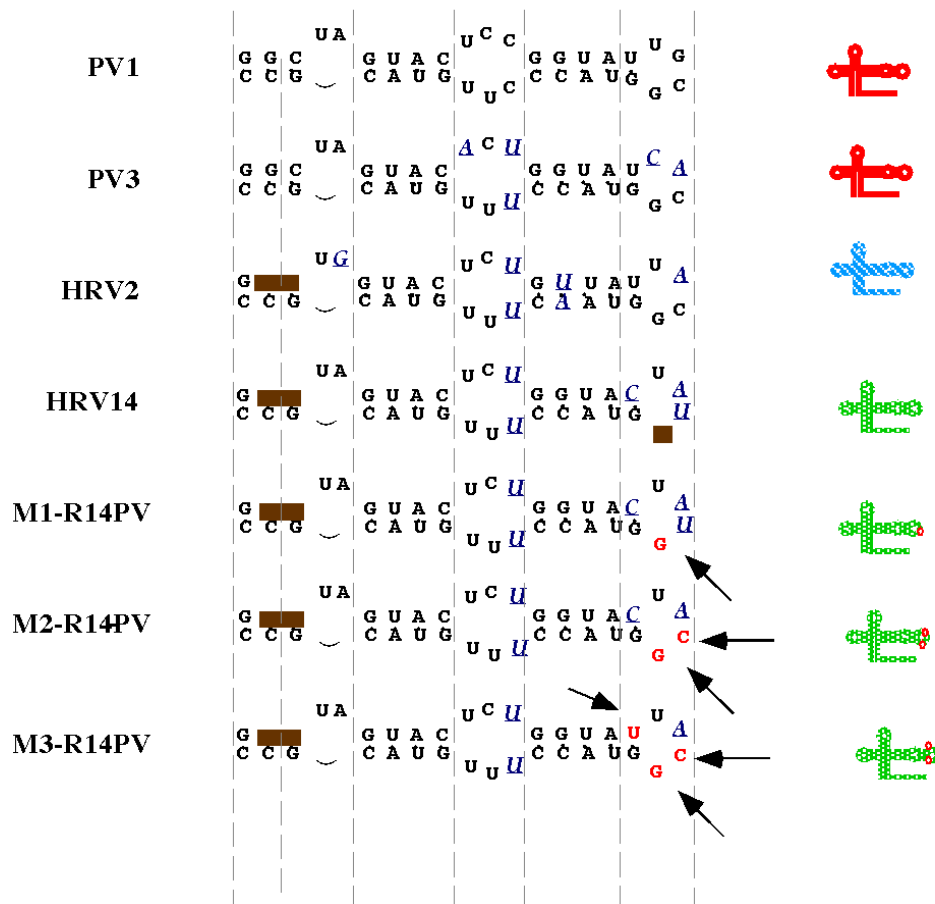
fold molar excess of tRNA (Fig. 3C, lane 12), a result that will be discussed later. Polypeptide 3AB is a non-specific RNA-binding protein (Paul *et al.*, 1994). Accordingly, all three RNA probes bound 3AB equally well in the absence of competitor tRNA (Fig. 3C, lanes 7–9). This binding, however, was abolished in the presence of competitor tRNA (data not shown; see also Fig. 6). These properties demonstrate further that 3AB only engages in the formation of the ternary complex after 3CD^{pro} has recognized the CL RNA (Harris *et al.*, 1994; Xiang *et al.*, 1995a, b).

Fine mapping of the HRV14 stem–loop D CL sequences that restore genome replication

A comparison of the sequences of subdomain D of CL elements of PVs and HRVs (Fig. 4A), together with considerations of replication phenotypes in the context of PV1(M), suggested that the loop of subdomain D (Fig. 4B) may harbour an important function in protein binding. The absence of one nucleotide in the loop is the most striking difference between the HRV14 subdomain D and the other subdomain D loops. To determine the sequence requirement in this region of PV replication, we have altered the sequence of the loop in subdomain D of the HRV14 CL. The effects of mutations were assayed in chimeric constructs consisting of the PV1(M) genome in which the cognate CL was exchanged with that of HRV14 (R14/PV).

Insertion of a G residue at position 61 ($C_{57}UAU_{60}GG_{61}$; M1-R14PV) yielded a non-viable chimeric genome when transfected into HeLa cells (Fig. 5A). No virus was isolated even after 4 days of incubation and blind passages. We then changed the U_{60} residue to a C ($C_{57}UAC_{60}GG_{61}$), since a C is found in this position in CL elements compatible with PV replication (Fig. 4B). Indeed, in the context of the chimeric virus, this altered D loop ($CUAC_{60}GG_{61}$) rescued replication (Fig. 5A, M2-R14PV). A third mutation in the HRV14 D loop, a substitution of C_{57} with U ($U_{57}UAC_{60}GG_{61}$; M3-R14PV), had little effect on virus replication (Fig. 5A; and see below).

A.



B.

		Ternary complex formation	Growth Phenotypes	
	PV1 (M) :	UUGCGG	+++	++
	PV2 (L) :	-C----	nd	++
	PV1 (s) :	-A----	nd	++
CBV3 →	PV3 (L) :	-CA----	nd	++
	HRV2 :	-A----	+	+
	HRV14 :	C-AU.-	-	-
	M1-R14PV:	C-AU.-	+	-
	M2-R14PV:	C-A----	++	+
	M3-R14PV:	--A----	++	+
	Consensus:	Y ^Y R ^Y C ^Y G ^Y G ^Y		

Tetra loop

Fig. 4. (A) Detailed alignment of subdomain D from PV1, PV3, HRV2 and HRV14, and the mutants used in this study. Filled rectangles represent the PV1 sequences absent in HRV2 and HRV14. Underlined letters display the nucleotide differences between homologous PV1 and the others. Arrows indicate the location of changes introduced into the HRV14 CL. PV1 and PV3 stem-loop D is illustrated on the right-hand-side in red, HRV2 in blue and HRV14 in green. The locations of the changes in the HRV14 stem-loop D are shown. (B) Nucleotide sequence alignment of loop residues within subdomain D of homologous CLs, their phenotypes and the summary of results of RNA-protein-binding assays. The numbering of each subdomain D is indicated in Fig. 1(A). Boxed sequences indicate the tetra loop in subdomain D. The consensus sequence is shown at the bottom; it indicates the degree of conservation at each nucleotide position: R, purine; Y, pyrimidine. A dot indicates the absence of that particular nucleotide. '+' and '-', phenotype (viability); nd, not determined.

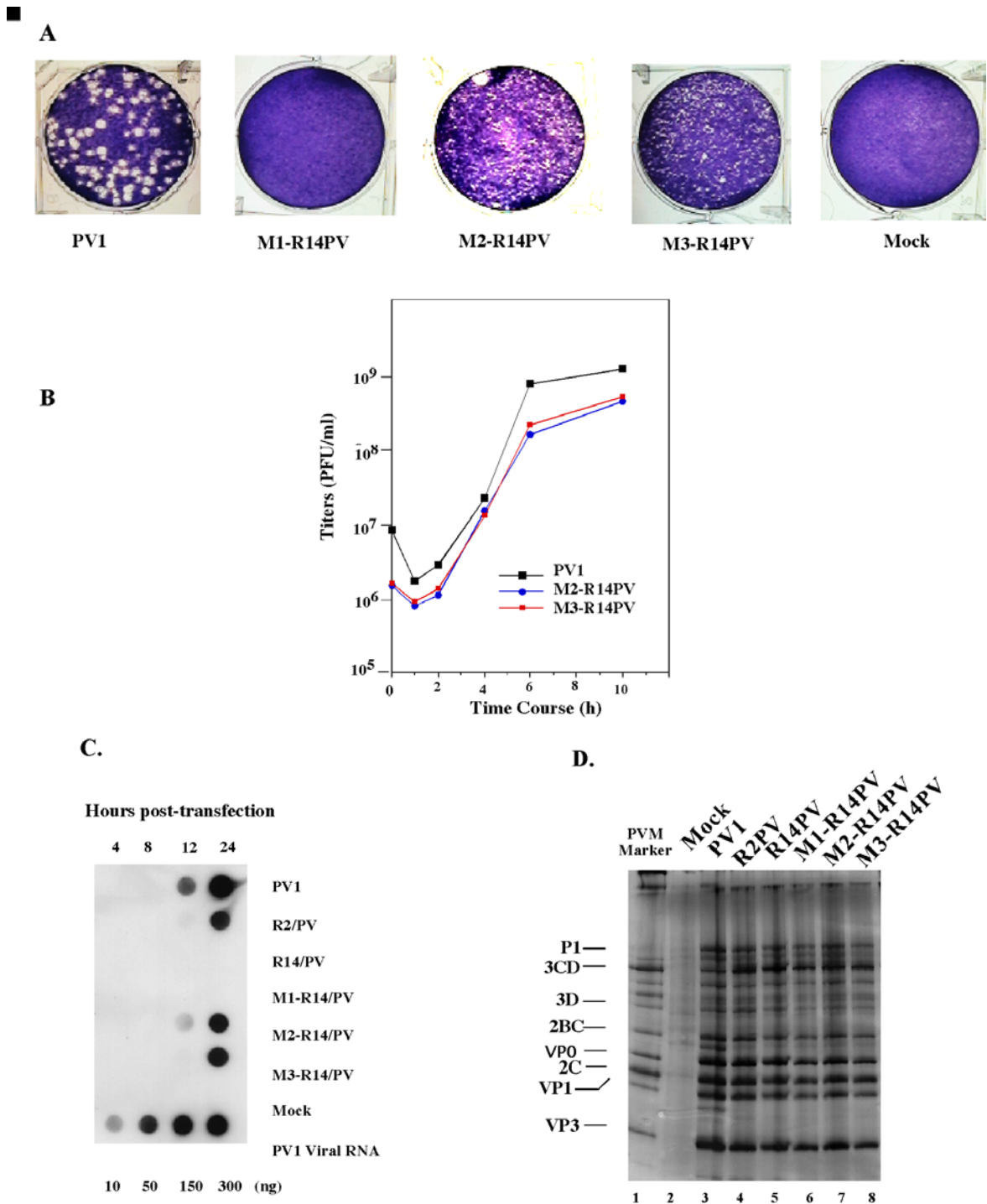


Fig. 5. Effect of mutations within subdomain D of the HRV14 CL on the viability of R14PV chimeric RNAs. (A) Plaque phenotype of virus derived from wt and R14PV mutant transcript RNAs. (B) One-step growth curves of PV wt and two viable mutant viruses of R14PV. HeLa cell monolayers were infected at an m.o.i. of 5. At various times post-infection, cells were harvested and virus titres were determined by plaque assay on HeLa cells, as indicated in Methods. Results were calculated from duplicate wells frozen at each time-point. (C) Measurement of plus-strand RNA synthesis by dot-blot hybridization analyses. The bottom panel contained increasing amounts of transcript PV1 RNA as a control for quantification. (D) *In vitro* translation of wt and chimeric CL RNAs. Reaction mixtures containing no viral RNA (mock) or *in vitro*-transcribed R2PV, R14PV mutants (M1, M2 and M3) and wt PV RNAs (200 ng) were translated in a HeLa S10 cell extract at 30 °C overnight and analysed on a 12.5 % polyacrylamide gel. [³⁵S]Methionine-labelled PV1(M) proteins from infected HeLa cells were used as a marker.

Compared to wt PV1(M), the viruses derived from the M2-R14PV and M3-R14PV RNAs expressed a small plaque phenotype that was maintained through four additional passages (Fig. 5A). Sequence analysis of RT-PCR products corresponding to RNA extracted from the first and the fourth passage viruses showed that the mutations introduced were still present after four passages and no additional mutations (within the 5'NTR and 3CD^{pro} regions) were found.

The growth characteristics of viruses M2-R14PV and M3-R14PV were investigated by performing a one-step growth experiment. HeLa R19 cells were infected with viruses and titres were determined by plaque assay at different times (Fig. 5B). Although the replication kinetics of wt and mutant chimeric viruses are similar, the yield of the mutant viruses was reduced. This apparent phenotype in virus yield was mirrored by a non-radioactive RNA hybridization assay, performed to detect plus-strand RNA. For this purpose, plus-strand RNA synthesis was monitored at different times after transfection of PV1(M), R2/PV, M2-R14PV, M3-R14PV, R14/PV or M1-R14PV RNAs into HeLa cell monolayers. The signal indicating synthesis of PV1(M), R2/PV, M2-R14PV and M3-R14PV genomes increased over time (Fig. 5C). In contrast, no plus-strand RNA synthesis could be detected in cells transfected with either R14/PV or M1-R14PV RNAs. The reduced signal for the R2/PV, M2-R14PV and M3-R14PV genomes may be the reason for the reduced yield of the respective viruses. These results show that the lethal phenotype of R14/PV and M1-R14PV genomes is related to a defect in RNA synthesis.

A translation phenotype has been reported as the result of an insertion mutation into the CL of PV1(M) (Simoes & Sarnow, 1991). Therefore, it could be argued that the abrogation of replication of the R14/PV and M1-R14PV genomes is due to aberrant protein synthesis and/or proteolytic processing. To test this possibility, we performed RNA translation assays. Full-length PV1(M) and chimeric RNA transcripts were translated using a HeLa cell-free extract (Molla *et al.*, 1991). Neither the relative translation efficiencies nor the processing levels were altered due to sequence differences in the CLs (Fig. 5D), an observation ruling out an indirect effect of polyprotein processing for the lack of replication of the R14/PV and M1-R14PV genomes.

Ternary complexes formed between 3CD^{pro}-3AB and 3CD^{pro}-PCBP proteins with wt and mutant HRV14 CLs

To investigate to what extent wt or mutant HRV14 CL elements are capable of RNP formation with 3CD^{pro} and 3AB or 3CD^{pro} and PCBP2, [α -³²P]UTP-labelled CL probes were synthesized *in vitro*. Recombinant PCBP2, 3AB and 3CD^{pro}, alone or in combination, were incubated with plus-strand riboprobes in a binding reaction containing a 1000-fold molar excess of tRNA. The protein-RNA complexes were then examined in non-denaturing gels by EMSA (Fig. 6). Both 3CD^{pro}-3AB and 3CD^{pro}-PCBP2 formed ternary complexes efficiently with the CLs of PV1, HRV2, M2-R14PV and M3-R14PV

transition at position 57 had little effect on replication (Fig. 6, lanes 34 and 35). The latter is not surprising, since the D loop of M3-R14PV CL is identical to that of the CL of HRV2 (Fig. 4B). As we have reported previously, the replacement of the cognate PV1(M) CL with that of HRV2 CL also yields a replication phenotype (Xiang *et al.*, 1995b). We conclude that the consensus sequence in the D loop, as required for function in the context of PV proteins, is YYRCGG (the sequence underlined represents a tetra loop).

CL and PV*cre*(2C) RNA signals appear to function independently from each other

Previous studies have suggested that CL and PV*cre*(2C), a *cis* replication signal encoded in the PV P2 region (Gamarnik & Andino, 1998; Goodfellow *et al.*, 2000; Paul *et al.*, 2000; Rieder *et al.*, 2000), are essential for minus-strand RNA synthesis in PV replication. As pointed out before, available evidence suggests that these RNA elements accomplish their function via the formation of RNP complexes, both depending stringently upon 3CD^{pro}. Does the CL–RNP cross-talk with the *cre*–RNP complex in VPg uridylylation? To answer this question, we examined VPg uridylylation *in vitro* in the context of the PV chimera R14PV. Specifically, we analysed whether the inability of the HRV14 CL in R14PV to form an RNP with 3CD^{pro}–3AB or 3CD^{pro}–PCBP2 has any effect on the template function provided by PV*cre*(2C). *In vitro* VPg-uridylylation reactions using 3D^{pol}, 3CD^{pro}, UTP/Mg²⁺ and VPg with full-length viral RNA templates were carried out as described previously (Paul *et al.*, 2000; Rieder *et al.*, 2000). PV*cre*(2C)-dependent VPg uridylylation with chimeric RNAs as templates was as efficient as that with wt PV1(M) RNA and it was dependent strictly on the presence of 3CD^{pro} (Fig. 7). Thus, the replacement of CL elements at the 5'NTR by competent or non-functional structures did not result in any appreciable change in the overall PV*cre*(2C) activity as a template in the uridylylation reaction of VPg. These results suggest that the CL and PV*cre*(2C) elements function as two independent domains in their role in virus RNA replication.

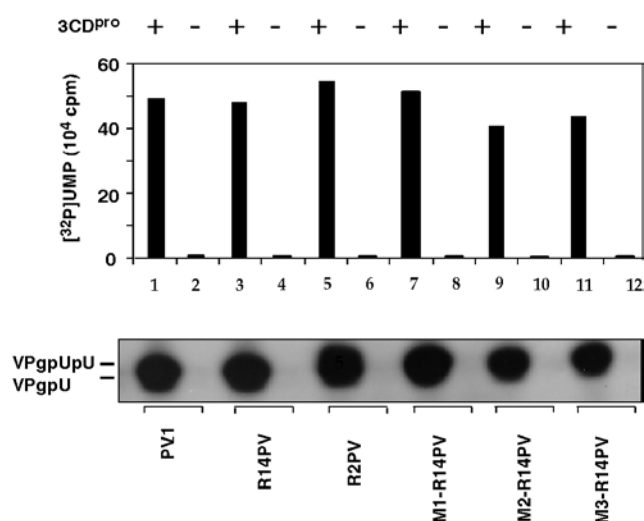


Fig. 7. Uridylylation of VPg using full-length transcript RNAs as templates for the reaction. The uridylylation of VPg by 3D^{pol} was measured with the standard assay as described in Methods. An autoradiograph of the reaction products is shown in the bottom panel; quantification of the data is displayed above.

DISCUSSION

Currently, there are four structural elements in PV RNA that have been implicated firmly in genome replication: 5'-terminal CL, *cre*(2C), 3' non-coding heteropolymeric region and 3'-terminal poly(A) tail (Agol *et al.*, 1999; Paul, 2002; Xiang *et al.*, 1997; and references therein). In addition, genetic evidence has been interpreted to mean that the PV IRES is also involved in RNA synthesis (Borman *et al.*, 1994; Shiroki *et al.*, 1995). This, however, is difficult to comprehend in view of chimeric PV genomes in which the cognate IRES was replaced with that of hepatitis C virus (Zhao & Wimmer, 2001). The mechanism of function in PV RNA synthesis has only been elucidated for *cre*(2C). This element is the template in the uridylylation of VPg, the product of which (VPgpUpU) is the primer for the RNA polymerase in the initiation of RNA synthesis (Gerber *et al.*, 2001; Paul *et al.*, 1998, 2000, 2003; Rieder *et al.*, 2000; Yin *et al.*, 2003).

Based on genetic and biochemical analyses, a function of the 5'-terminal CL in PV RNA replication was proposed first by Andino *et al.* (1993). These authors found that the CL can form an RNP with PV 3CD^{pro} and a 'host factor', identified later as PCBP2 (Blyn *et al.*, 1996; Gamarnik & Andino, 1997; Parsley *et al.*, 1997). Originally, it was suggested that the 5'-terminal CL RNP plays a role in the initiation of plus-strand RNA synthesis (Andino *et al.*, 1993). Recently, however, the importance of this complex has been shifted to the initiation of minus-strand RNA synthesis via the formation of a circular plus-strand template (Barton *et al.*, 2001; Herold & Andino, 2001; Teterina *et al.*, 2001; Paul, 2002). Circularization has been proposed to be mediated through the affinity of the poly(A)-associated poly(A)-binding protein (PABP) to the CL-bound 3CD^{pro} and PCBP. Whatever the role of the CL, the viral proteinase 3CD^{pro}, which is also an RNA-binding protein (Andino *et al.*, 1993; Harris *et al.*, 1994), is the key in the specific recognition of the 5'-terminal RNA structure.

Whereas the cellular protein PCBP2 forms a specific ternary complex with CL–3CD^{pro} (Gamarnik & Andino, 1997, 2000; Parsley *et al.*, 1997; Walter *et al.*, 2002), it can be replaced with the virus-specific protein 3AB (Harris *et al.*, 1994; Xiang *et al.*, 1995a, b), a non-specific RNA-binding protein (Paul *et al.*, 1994) and the precursor for VPg. Indeed, in the presence of a 1000-fold molar excess of tRNA, the formation of the ternary complex CL–3CD^{pro}–3AB is highly specific. Its significance has been supported by genetic and biochemical analyses that included different CL elements (Xiang *et al.*, 1995b) and numerous mutants of 3AB (Xiang *et al.*, 1995a). Importantly, a failure to form the CL–3CD^{pro}–3AB complex *in vitro* co-varies in all cases with a lethal replication phenotype *in vivo* (Xiang *et al.*, 1995a, b).

An exchange of the cognate CL of PV1(M) with that of HRV2 yields a virus with a replication phenotype (Xiang *et al.*, 1995b). The HRV14 CL, on the other hand, cannot substitute for the PV CL (Rohll *et al.*, 1994; Xiang *et al.*, 1995b). Superficially, the three CL elements have similar structures (Fig. 1A–C).

There are, however, many differences, as, for example, the deletions in the HRV CLs relative to the PV CL. However, in the context of PV replication, the integrity of the short stem (D1) at the bottom of subdomain D (Fig. 1, compare A with B and C) cannot be essential because the HRV2/PV1(M) chimera can replicate and produce virus (Fig. 2B) (Xiang *et al.*, 1995b). Similarly, the deletion of two nucleotides in the loop of subdomain B of the HRV14 CL cannot have a lethal effect in the context of a replicating PV genome. This is because a chimeric CL consisting of subdomains A, B and C of HRV14 and subdomain D of PV3(L) (Fig. 1D), when placed to the 5' end of a PV3(L) replicon (Rohll *et al.*, 1994) or PV genome, promoted RNA synthesis, albeit poorly (Figs 2 and 3). Unexpectedly, both the dicistronic and the monocistronic PV1(M) genomes carrying the chimeric CLC were not only debilitated in replication at 37 °C but also expressed a strong *ts* phenotype. The reason for this phenotype is obscure. A *ts* phenotype has been observed for some other 5' chimeras before (Johnson & Semler, 1988; Zell *et al.*, 1995).

To determine the molecular basis for the failure of the HRV14 CL to substitute for the PV CL, we have changed the sequence of the HRV14 CL by site-directed mutagenesis. Based on the data described above, it was highly likely that the subdomain D within the HRV14 CL is the culprit of malfunction. A comparison of different PV and HRV subdomain D structures (Fig. 4A) revealed a consensus sequence in the loop (Fig. 4B) that was highly likely to play a major role in CL function. This loop consensus sequence, YYRCGG (the underlined residues forming a tetra loop; Fig. 1), is identical to that proposed recently by Zell *et al.* (2002). In contrast, the loop sequence in subdomain D of HRV14 is shorter by one residue (CUAU◆G) (Fig. 4B). Insertion of a G residue to yield the sequence CUAUGG, however, was not sufficient to rescue the genome replication of the HRV14/PV chimera (M1-R14PV). According to the studies of Zell *et al.* (2002), the mere presence of a tetra loop in subdomain D (as indicated by the underlined sequence in CUAUGG), but not its sequence, is sufficient to form a complex between CL and the viral RNA-binding protein 3C^{pro}. However, binding of 3CD^{pro} alone is not sufficient to restore the replication competence of M1-R14PV and this issue is discussed below. Further mutagenesis of the loop region of the HRV14 subdomain D to yield CUACGG generated a chimeric genome (M2-R14PV) that replicated efficiently, albeit slightly slower than wt PV1(M). An additional mutation to UUACGG (M3-R14PV), leading to a sequence identical to that of the Sabin strain of PV2 [PV2(S)], did not improve virus replication. It is likely that the replication phenotypes of M2-R14PV and M3-R14PV are related to the sequences (and structures) of the HRV14 CL in stem-loops A–C. These subdomains are quite different from that of PV. This hypothesis is supported by the observation that the chimeric HRV2/PV genome, having the identical loop sequence in subdomain D of its HRV2 CL as PV1(S), also expresses a replication phenotype (Xiang *et al.*, 1995b).

The likely reason for the lethal phenotype of the HRV14/PV chimera R14/PV is the failure of the HRV14 CL to form ternary complexes with either 3CD^{pro}-3AB or 3CD^{pro}-PCBP2. Fittingly, mutagenesis of the loop region of the HRV14 subdomain D that led to the rescue of replication also generated CL structures capable of interacting with the RNA-binding proteins (Fig. 6). However, the generation of a tetra loop in subdomain D of M1-R14PV did produce only patterns of very weak protein binding (Fig. 6, lanes 20–23). Significantly, M1-R14PV failed to generate viable virus. Thus, a tetra loop per se in the HRV14 CL subdomain D is not sufficient for replication function in this system. Although Zell *et al.* (2002) elegantly showed that subdomain D of the HRV14 CL carrying an engineered tetra loop could bind to CVB3 3C^{pro}, the RNA-binding moiety of 3CD^{pro}, binding of a protein to this domain is not sufficient for the replication function of the CL element. An additional mutation in the tetra loop of M1-R14PV was necessary to effect significant ternary complex formation, that is, recruit the third binding partner 3AB or PCBP2 (Fig. 6, lanes 26–29). Accordingly, this CL promotes replication of M2-R14PV.

Tetra loops formed by single-strand RNAs are exceptionally stable, presumably because they form complex higher order structures. These structures vary with the sequence of the tetra loop (Nowakowski & Tinoco, 1997). There are several tetra loop families known, of which one has the sequence UNCG, the sequence in subdomain D of PV1(M). In this tetra loop, the C base forms an important hydrogen bond with the phosphate on the 3' side of the U nucleotide (Allain & Varani, 1995). In M1-R14PV, this requirement is not fulfilled. However, a tetra loop with the sequence UNCG has been generated in M2-R14PV (CUAUGG→CUACGG), the C residue 5' adjacent to the G residue being essential. Thus, in variance of the conclusions by Zell *et al.* (2002), we propose that the sequence and, consequently the structure, of the loop in domain D of the CL plays an additional important role in signalling initiation of RNA synthesis. Of course, the tetra loop (CNCG) in the CL of PV2(L) and PV3(L) (Fig. 4B) is slightly different than the tetra loop of PV1(M) (UNCG), yet it functions efficiently, even in serotype chimeras (for example, in recombinants between serotypes). Moreover, tetra loops in subdomain D of CL elements are clearly not essential for some members of the genus *Rhinovirus*, as, for example, HRV14. The HRV14 replication proteins are perfectly happy with the small loop in subdomain D of their CL. It is noteworthy that the HRV14 replication proteins are also perfectly happy with a PV1(M) CL carrying a tetra loop. Todd *et al.* (1997) reported that a chimeric genome in which the entire 5'-terminal NTR of PV was spliced onto the ORF and 3'NTR of HRV14 replicated as efficiently as the parental HRV14. These considerations underline the complexity of the structure/function relationships in PV RNA replication (Agol *et al.*, 1999).

To what extent the structure of the stem domains of subdomain D in the HRV14 CL play a role in protein binding remains to be seen (Walker *et al.*, 1995). In the context of the PV1(M) replication machinery, these domains appear to play a minor role.

It should be noted that the CL in natural plus-strand template RNAs is linked covalently at the 5' end to VPg (VPgpUpU) (Lee *et al.*, 1977; Wimmer *et al.*, 1993). In PV protein synthesis, all viral (genome-length) mRNA has been separated from VPg by a cellular phosphodiesterase (Gulevich *et al.*, 2002; Hewlett *et al.*, 1976; Nomoto *et al.*, 1976) and, thus, has a 5'-terminal pUU. It is not clear whether the incoming, infecting genomic RNA undergoes this modification also. RNA free of VPg is infectious, but the specific infectivity of such RNA, for example, transcript RNAs derived from plasmids, is lower by as much as one order of magnitude as compared to VPg-linked virion RNA. This is true even if the transcript RNA, synthesized with phage T7 RNA polymerase (van der Werf *et al.*, 1986), carries a ribozyme moiety at the 5' end, thereby yielding mostly a pUU terminus (Herold & Andino, 2000; D. W. Kim & E. Wimmer, unpublished results). All biochemical studies of ternary complex formation have been carried out with CL RNAs synthesized with T7 RNA polymerase. Thus, these riboprobes are not covalently linked to VPg. Consider that the C-terminal VPg portion of 3AB (3B=VPg) is responsible for the RNA-binding activity of 3AB (Xiang *et al.*, 1995a). It is not known to what extent the covalent attachment of VPg to the CL influences ternary complex formation. Could it be that VPg-linked CLs can form complexes with 3CD^{pro}, for example, 3CD^{pro}-VPg-CL, which would be necessary *and* sufficient to promote RNA replication? If so, the formation of CL-3CD^{pro}-PCBP2 or CL-3CD^{pro}-3AB complexes may be important only during a specific phase in replication, perhaps in the very initial phase. Currently, this important problem cannot be solved because sufficient quantities of VPg-linked CL cannot be synthesized *in vitro*. We have ignored this fascinating question in this study also.

The first step in PV RNA synthesis is the uridylylation of VPg by 3D^{pol}, a reaction that provides the primer for the RNA polymerase. The reaction requires a *cis*-acting replication signal, termed *cre*, and has been identified in all picornaviral RNAs analysed so far (Gerber *et al.*, 2001; Goodfellow *et al.*, 2000; Lobert *et al.*, 1999; Mason *et al.*, 2002; McKnight & Lemon, 1996, 1998). Interestingly, *cre* elements in PV RNA are located at vastly different positions within the viral genome. In PV, the *cre*(2C) maps to the coding region of the viral protein 2C^{ATPase} (Goodfellow *et al.*, 2000). Functional *cre* elements can be moved within the PV genome to very different locations, even between the CL and the IRES (Yin *et al.*, 2003). Available evidence suggests that the sole function of the *cre* element is to serve as specific template in the uridylylation of VPg (Paul *et al.*, 2000; Rieder *et al.*, 2000). Importantly, *cre*-dependent uridylylation requires 3CD^{pro} as a co-factor, just like the function of the 5'-terminal CL. It is interesting to point out that our *in vitro* experiments of VPg uridylylation contrast with some studies reported by Lyons *et al.* (2001) using the translation/replication system. Those results indicate that the CL is important for VPg uridylylation and minus-strand RNA synthesis. Considering the proposed, complex circular RNA structure involved in the initiation of PV RNA synthesis, it seems possible that the protein complex formed in *cre*-dependent uridylylation may interact functionally with the RNP formed at the 5'-terminal CL. The data presented here suggest that *cre* and CL function independently from each other.

ACKNOWLEDGEMENTS

We thank D. W. Kim for supplying recombinant His-tagged 3CD^{pro} and T. Pfister for plasmid pBS-2C. Our gratitude goes to B. Semler for providing a PCBP-expression vector. This work was supported by grant AI15122 of the National Institute of Allergy and Infectious Diseases.

REFERENCES

- Agol, V. I., Paul, A. V. & Wimmer, E. (1999).** Paradoxes of the replication of picornaviral genomes. *Virus Res* **62**, 129–147.
- Alexander, L., Lu, H. H. & Wimmer, E. (1994).** Polioviruses containing picornavirus type 1 and/or type 2 internal ribosomal entry site elements: genetic hybrids and the expression of a foreign gene. *Proc Natl Acad Sci U S A* **91**, 1406–1410.
- Allain, F. H. & Varani, G. (1995).** Divalent metal ion binding to a conserved wobble pair defining the upstream site of cleavage of group I self-splicing introns. *Nucleic Acids Res* **23**, 341–350.
- Andino, R., Rieckhof, G. E. & Baltimore, D. (1990).** A functional ribonucleoprotein complex forms around the 5' end of poliovirus RNA. *Cell* **63**, 369–380.
- Andino, R., Rieckhof, G. E., Achacoso, P. L. & Baltimore, D. (1993).** Poliovirus RNA synthesis utilizes an RNP complex formed around the 5'-end of viral RNA. *EMBO J* **12**, 3587–3598.
- Barton, D. J., O'Donnell, B. J. & Flanagan, J. B. (2001).** 5' cloverleaf in poliovirus RNA is a *cis*-acting replication element required for negative-strand synthesis. *EMBO J* **20**, 1439–1448.
- Blair, W. S., Parsley, T. B., Bogerd, H. P., Towner, J. S., Semler, B. L. & Cullen, B. R. (1998).** Utilization of a mammalian cell-based RNA binding assay to characterize the RNA binding properties of picornavirus 3C proteinases. *RNA* **4**, 215–225.
- Blyn, L. B., Swiderek, K. M., Richards, O., Stahl, D. C., Semler, B. L. & Ehrenfeld, E. (1996).** Poly(rC) binding protein 2 binds to stem-loop IV of the poliovirus RNA 5' noncoding region: identification by automated liquid chromatography-tandem mass spectrometry. *Proc Natl Acad Sci U S A* **93**, 11115–11120.
- Borman, A. M., Deliat, F. G. & Kean, K. M. (1994).** Sequences within the poliovirus internal ribosome entry segment control viral RNA synthesis. *EMBO J* **13**, 3149–3157.
- Cornell, C. T. & Semler, B. L. (2002).** Subdomain specific functions of the RNA polymerase region of poliovirus 3CD polypeptide. *Virology* **298**, 200–213.
- Gamarnik, A. V. & Andino, R. (1997).** Two functional complexes formed by KH domain containing proteins with the 5' noncoding region of poliovirus RNA. *RNA* **3**, 882–892.
- Gamarnik, A. V. & Andino, R. (1998).** Switch from translation to RNA replication in a positive-stranded RNA virus. *Genes Dev* **12**, 2293–2304.
- Gamarnik, A. V. & Andino, R. (2000).** Interactions of viral protein 3CD and poly(rC) binding protein with the 5' untranslated region of the poliovirus genome. *J Virol* **74**, 2219–2226.
- Gerber, K., Wimmer, E. & Paul, A. V. (2001).** Biochemical and genetic studies of the initiation of human rhinovirus 2 RNA replication: identification of a *cis*-replicating element in the coding sequence of 2A^{pro}. *J Virol* **75**, 10979–10990.
- Goodfellow, I., Chaudhry, Y., Richardson, A., Meredith, J., Almond, J. W., Barclay, W. & Evans, D. J. (2000).** Identification of a *cis*-acting replication element within the poliovirus coding region. *J Virol* **74**, 4590–4600.
- Gulevich, A. Y., Yusupova, R. A. & Drygin, Y. F. (2002).** VPg unlinkase, the phosphodiesterase that hydrolyzes the bond between VPg and picornavirus RNA: a minimal nucleic moiety of the substrate. *Biochemistry* **67**, 615–621.
- Harris, K. S., Xiang, W., Alexander, L., Lane, W. S., Paul, A. V. & Wimmer, E. (1994).** Interaction of poliovirus polypeptide 3CD^{pro} with the 5' and 3' termini of the poliovirus genome. Identification of viral and cellular cofactors needed for

efficient binding. *J Biol Chem* **269**, 27004–27014.

Herold, J. & Andino, R. (2000). Poliovirus requires a precise 5' end for efficient positive-strand RNA synthesis. *J Virol* **74**, 6394–6400.

Herold, J. & Andino, R. (2001). Poliovirus RNA replication requires genome circularization through a protein–protein bridge. *Mol Cell* **7**, 581–591.

Hewlett, M. J., Rose, J. K. & Baltimore, D. (1976). 5'-Terminal structure of poliovirus polyribosomal RNA is pUp. *Proc Natl Acad Sci U S A* **73**, 327–330.

Johnson, V. H. & Semler, B. L. (1988). Defined recombinants of poliovirus and coxsackievirus: sequence-specific deletions and functional substitutions in the 5'-noncoding regions of viral RNAs. *Virology* **162**, 47–57.

Kusov, Y. Y. & Gauss-Muller, V. (1997). *In vitro* RNA binding of the hepatitis A virus proteinase 3C (HAV 3C^{pro}) to secondary structure elements within the 5' terminus of the HAV genome. *RNA* **3**, 291–302.

Lama, J., Paul, A. V., Harris, K. S. & Wimmer, E. (1994). Properties of purified recombinant poliovirus protein 3AB as substrate for viral proteinases and as co-factor for viral polymerase 3D^{pol}. *J Biol Chem* **269**, 66–70.

Larsen, G. R., Semler, B. L. & Wimmer, E. (1981). Stable hairpin structure within the 5'-terminal 85 nucleotides of poliovirus RNA. *J Virol* **37**, 328–335.

Lee, Y. F., Nomoto, A., Detjen, B. M. & Wimmer, E. (1977). The genome-linked protein of picornaviruses. I. A protein covalently linked to poliovirus genome RNA. *Proc Natl Acad Sci U S A* **74**, 59–63.

Leong, L. E., Walker, P. A. & Porter, A. G. (1993). Human rhinovirus-14 protease 3C (3C^{pro}) binds specifically to the 5'-noncoding region of the viral RNA. Evidence that 3C^{pro} has different domains for the RNA binding and proteolytic activities. *J Biol Chem* **268**, 25735–25739.

Lobert, P. E., Escriou, N., Ruelle, J. & Michiels, T. (1999). A coding RNA sequence acts as a replication signal in cardioviruses. *Proc Natl Acad Sci U S A* **96**, 11560–11565.

Lyons, T., Murray, K. E., Roberts, A. W. & Barton, D. J. (2001). Poliovirus 5'-terminal cloverleaf RNA is required in *cis* for VPg uridylylation and the initiation of negative-strand RNA synthesis. *J Virol* **75**, 10696–10708.

Mason, P. W., Bezborodova, S. V. & Henry, T. M. (2002). Identification and characterization of a *cis*-acting replication element (*cre*) adjacent to the internal ribosome entry site of foot-and-mouth disease virus. *J Virol* **76**, 9686–9694.

McKnight, K. L. & Lemon, S. M. (1996). Capsid coding sequence is required for efficient replication of human rhinovirus 14 RNA. *J Virol* **70**, 1941–1952.

McKnight, K. L. & Lemon, S. M. (1998). The rhinovirus type 14 genome contains an internally located RNA structure that is required for viral replication. *RNA* **4**, 1569–1584.

Molla, A., Paul, A. V. & Wimmer, E. (1991). Cell-free, *de novo* synthesis of poliovirus. *Science* **254**, 1647–1651.

Nomoto, A., Lee, Y. F. & Wimmer, E. (1976). The 5' end of poliovirus mRNA is not capped with m7G(5')ppp(5')Np. *Proc Natl Acad Sci U S A* **73**, 375–380.

Nowakowski, J. & Tinoco, I. (1997). RNA structure and stability. *Semin Virol* **8**, 153–165.

Parsley, T. B., Towner, J. S., Blyn, L. B., Ehrenfeld, E. & Semler, B. L. (1997). Poly(rC) binding protein 2 forms a ternary complex with the 5'-terminal sequences of poliovirus RNA and the viral 3CD proteinase. *RNA* **3**, 1124–1134.

Paul, A. V. (2002). Possible unifying mechanism of picornavirus genome replication. In *Molecular Biology of Picornaviruses*, p227–246. Edited by B. L. Semler and E. Wimmer. Washington: ASM Press.

Paul, A. V., Cao, X., Harris, K. S., Lama, J. & Wimmer, E. (1994). Studies with poliovirus polymerase 3D^{pol}. Stimulation of poly(U) synthesis *in vitro* by purified poliovirus protein 3AB. *J Biol Chem* **269**, 29173–29181.

Paul, A. V., van Boom, J. H., Filippov, D. & Wimmer, E. (1998). Protein-primed RNA synthesis by purified poliovirus RNA polymerase. *Nature* **393**, 280–284.

Paul, A. V., Rieder, E., Kim, D. W., van Boom, J. H. & Wimmer, E. (2000). Identification of an RNA hairpin in poliovirus

- RNA that serves as the primary template in the *in vitro* uridylylation of VPg. *J Virol* **74**, 10359–10370.
- Paul, A. V., Peters, J., Mugavero, J., Yin, J., van Boom, J. H. & Wimmer, E. (2003).** Biochemical and genetic studies of the VPg uridylylation reaction catalyzed by the RNA polymerase of poliovirus. *J Virol* **77**, 891–904.
- Pfister, T. & Wimmer, E. (1999).** Characterization of the nucleoside triphosphatase activity of poliovirus protein 2C reveals a mechanism by which guanidine inhibits poliovirus replication. *J Biol Chem* **274**, 6992–7001.
- Rieder, E., Paul, A. V., Kim, D. W., van Boom, J. H. & Wimmer, E. (2000).** Genetic and biochemical studies of poliovirus *cis*-acting replication element *cre* in relation to VPg uridylylation. *J Virol* **74**, 10371–10380.
- Rivera, V. M., Welsh, J. D. & Maizel, J. V., Jr (1988).** Comparative sequence analysis of the 5' noncoding region of the enteroviruses and rhinoviruses. *Virology* **165**, 42–50.
- Rohll, J. B., Percy, N., Ley, R., Evans, D. J., Almond, J. W. & Barclay, W. S. (1994).** The 5'-untranslated regions of picornavirus RNAs contain independent functional domains essential for RNA replication and translation. *J Virol* **68**, 4384–4391.
- Shiroki, K., Ishii, T., Aoki, T., Kobashi, M., Ohta, S. & Nomoto, A. (1995).** A new *cis*-acting element for RNA replication within the 5' noncoding region of poliovirus type 1 RNA. *J Virol* **69**, 6825–6832.
- Simoës, E. A. F. & Sarnow, P. (1991).** An RNA hairpin at the extreme 5' end of the poliovirus RNA genome modulates viral translation in human cells. *J Virol* **65**, 913–921.
- Teterina, N. L., Egger, D., Bienz, K., Brown, D. M., Semler, B. L. & Ehrenfeld, E. (2001).** Requirements for assembly of poliovirus replication complexes and negative-strand RNA synthesis. *J Virol* **75**, 3841–3850.
- Todd, S., Towner, J. S. & Semler, B. L. (1997).** Translation and replication properties of the human rhinovirus genome *in vivo* and *in vitro*. *Virology* **229**, 90–97.
- van der Werf, S., Bradley, J., Wimmer, E., Studier, F. W. & Dunn, J. J. (1986).** Synthesis of infectious poliovirus RNA by purified T7 RNA polymerase. *Proc Natl Acad Sci U S A* **83**, 2330–2334.
- Walker, P. A., Leong, L. E. C. & Porter, A. G. (1995).** Sequence and structural determinants of the interaction between the 5'-noncoding region of picornavirus RNA and rhinovirus protease 3C. *J Biol Chem* **270**, 14510–14516.
- Walter, B. L., Parsley, T. B., Ehrenfeld, E. & Semler, B. L. (2002).** Distinct poly(rC) binding protein KH domain determinants for poliovirus translation initiation and viral RNA replication. *J Virol* **76**, 12008–12022.
- Wimmer, E. (1997).** Recognition signals on RNA genomes. *Semin Virol* **8**, 151–152.
- Wimmer, E., Hellen, C. U. T. & Cao, X. M. (1993).** Genetics of poliovirus. *Annu Rev Genet* **27**, 353–436.
- Xiang, W., Cuconati, A., Paul, A. V., Cao, X. & Wimmer, E. (1995a).** Molecular dissection of the multifunctional poliovirus RNA-binding protein 3AB. *RNA* **1**, 892–904.
- Xiang, W., Harris, K. S., Alexander, L. & Wimmer, E. (1995b).** Interaction between the 5'-terminal cloverleaf and 3AB/3CD^{pro} of poliovirus is essential for RNA replication. *J Virol* **69**, 3658–3667.
- Xiang, W., Paul, A. V. & Wimmer, E. (1997).** RNA signals in entero- and rhinovirus genome replication. *Rec Sig RNA Gen* **8**, 256–273.
- Yin, J., Paul, A. V., Wimmer, E. & Rieder, E. (2003).** Functional dissection of a poliovirus *cis*-acting replication element [PV-*cre*(2C)]: analysis of single- and dual-*cre* viral genomes and proteins that bind specifically to PV-*cre* RNA. *J Virol* **77**, 5152–5166.
- Zell, R., Klingel, K., Sauter, M., Fortmuller, U. & Kandolf, R. (1995).** Coxsackieviral proteins functionally recognize the polioviral cloverleaf structure of the 5'-NTR of a chimeric enterovirus RNA: influence of species-specific host cell factors on virus growth. *Virus Res* **39**, 87–103.
- Zell, R., Sidigi, K., Henke, A., Schmidt-Brauns, J., Hoey, E., Martin, S. & Stelzner, A. (1999).** Functional features of the bovine enterovirus 5'-non-translated region. *J Gen Virol* **80**, 2299–2309.
- Zell, R., Sidigi, K., Bucci, E., Stelzner, A. & Gorlach, M. (2002).** Determinants of the recognition of enteroviral cloverleaf

RNA by coxsackievirus B3 proteinase 3C. *RNA* **8**, 188–201.

Zhao, W. D. & Wimmer, E. (2001). Genetic analysis of a poliovirus/hepatitis C virus chimera: new structure for domain II of the internal ribosomal entry site of hepatitis C virus. *J Virol* **75**, 3719–3730.
